Density of states and supercurrent in diffusive SNS junctions: role of nonideal interfaces and spin-flip scattering

J.C. Hammer,[1,2] J.C. Cuevas,[3,2,4] F.S. Bergeret,[3] and W. Belzig[1]

[1] *Fachbereich Physik, Universität Konstanz, D-78457 Konstanz, Germany*
[2] *Institut für Theoretische Festkörperphysik, Universität Karlsruhe, D-76128 Karlsruhe, Germany*
[3] *Departamento de Física Teórica de la Materia Condensada, Universidad Autónoma de Madrid, E-28049 Madrid, Spain*
[4] *Forschungszentrum Karlsruhe, Institut für Nanotechnologie, D-76021 Karlsruhe, Germany*

We present a theoretical study of the density of states and supercurrent in diffusive superconductor-normal metal-superconductor (SNS) junctions. In particular, we study the influence on these two equilibrium properties of both an arbitrary transparency of the SN interfaces and the presence of spin-flip scattering in the normal wire. We show that the minigap that is present in the spectrum of the diffusive wire is very sensitive to the interface transmission. More importantly, we show that at arbitrary transparency the minigap replaces the Thouless energy as the relevant energy scale for the proximity effect, determining for instance the temperature dependence of the critical current. We also study in detail how the critical current is suppressed by the effect of spin-flip scattering, which can be due to either magnetic impurities or, under certain circumstances, to an external magnetic field. Our analysis based on the quasiclassical theory of diffusive superconductors can be very valuable to establish quantitative comparisons between experiment and theory.

I. INTRODUCTION

When a normal metal (N) and a superconductor (S) are brought together, their mutual interaction results in the modification of their electronic and transport properties. In particular, the normal metal may acquire genuine superconducting properties such a gap in the density of states or the ability to sustain a supercurrent. This effect, known as *proximity effect*, was first discussed by de Gennes[1] in the 1960's and in recent years it has been extensively studied in diffusive hybrid nanostructures.[2] Many equilibrium[3,4] and transport properties[5,6] of diffusive SN systems are now well understood, which is partially due to the impressive predictive power of the quasiclassical theory of superconductivity for diffusive systems, which is summarized in the Usadel equations.[7]

The proximity effect is mediated by Andreev reflections.[8] In this tunneling process an electron coming from N with energy ϵ below the superconducting gap Δ is converted into a reflected hole, thus transferring a Cooper pair to the S electrode. The time-reversed states involved in this process are coherent over a distance $L_C = \min(\sqrt{\hbar D/\epsilon}, L_\phi)$, where D is the diffusion constant of N and L_ϕ is the phase coherence length. This coherence may also be altered by interactions that break the time-reversal symmetry such as those induced by paramagnetic impurities or an external magnetic field.

In this work we present a theoretical study of the density of states and the supercurent in diffusive SNS junctions. These quantities nicely reflect the proximity effect under equilibrium conditions. It was first shown by McMillan[9] that a diffusive normal metal in contact with a superconductor can develop a gap in its electronic spectrum, which is usually referred to as *minigap*. More recently the minigap has been studied by numerous authors, usually within the framework of the Usadel equations.[10,11,12,13,14] From the experimental point of view, the appearance of a minigap has been tested indirectly in several tunneling experiments (see for instance Refs. [15,16] an references therein).

On the other hand, the fact that a SNS junction can sustain a supercurrent is known since the first experiments performed with Pb-Cu-Pb sandwiches.[17,18] It was soon realized that the existence of a dissipationless current in these structures is possible due to the proximity effect.[1] Later on, a more systematic experimental study of the critical current in these hybrid structures was carried out with the help of diffusive SNS microbridges.[19,20] The results of these experiments were described by Likharev,[21] who made use of the Usadel equations in the high temperature regime ($\Delta \ll k_B T$). A more general study of the Josephson effect in diffusive SNS junctions was made in Ref. [22]. More recently, Dubos *et al.*[6] demonstrated that the full temperature dependence of the critical current of diffusive Nb-Cu-Nb junctions with highly-transparent interfaces could be quantitatively described by the quasiclassical theory.

Most of the theoretical work done on proximity effect has been focused in the case of either ideal (perfectly transmissive) SN interfaces or in the tunneling limit,[23,24,25] with some notable exceptions.[26] One of the two main goals of this paper is to study how the local density of states (DOS) and the supercurrent in diffusive SNS junctions is influenced by arbitrary transmission of the interfaces. This is an important issue, in particular, in order to be able to establish quantitative comparisons between theory an experiment, since in reality the mismacht of material parameters leads to a broad range of transmission through the SN interfaces. In particular, we shall discuss the following issues: (i) how the transmission determines the magnitude of the minigap and, in general, the shape of the DOS in the normal wire, both in the absence and in the presence of a supercurrent and

(ii) how a finite transmission modifies the current-phase relation and the critical current of these junctions. Our results, based on the quasiclassical theory, show that the minigap, which is reduced as the interface resistance increases, is the energy scale that controls, in particular, the magnitude and temperature dependence of the critical current. For ideal interfaces, this role is played by the Thouless energy $\epsilon_T = \hbar D/L^2$, where L is the length of the normal metal.

The second goal of our work is to study the role of spin-flip scattering in the local DOS and supercurrent of diffusive SNS junctions. This type of scattering, which can be induced by magnetic impurities or an external magnetic field, breaks the time reserval symmetry between the electrons in Cooper pairs and reduces the superconducting correlations.[27,28] Different authors[11,14,24,29,30] have studied the effect of spin-flip scattering in the properties of SN structures. However, basic quantities like the supercurrent in SNS structures have, to our knowledge, not yet been addressed. We present in this work a detailed study of the dependence of the critical current of a diffusive SNS on the strength of the spin-flip scattering for arbitrary range of parameters (length of the normal wire, temperature and interface resistance). Our predictions can tested experimentally by measuring the critical current in the presence of magnetic field since, as long as the normal wire is a thin film, the field acts simply as a pair-breaking mechanism.[11,28,31]

The rest of the paper is organized as follows. In the next section we describe the general formalism, based on the quasiclassical theory for diffusive superconductors, that allows us to compute the DOS and the supercurrent in diffusive SNS junctions for arbitrary length, temperature and interface transparency. Section III is devoted to the analysis of the local DOS in the normal wire in different situations. In section IV we discuss the results for the dependence of the supercurrent on the interface resistance, temperature and strength of the spin-flip scattering. Finally, we summarize our main conclusions in section V. In the Appendix A we describe our analytical results for the critical current in the limit of weak proximity effect and in Appendix B we include some numerical fits described in the previous sections.

II. QUASICLASSICAL GREEN'S FUNCTIONS FORMALISM

We consider the SNS junction represented schematically in Fig. 1, where N is a diffusive normal metal of length L coupled to two identical superconducting reservoirs with gap Δ. We assume that the transport is phase-coherent, i.e. $L \ll L_\phi$ and neglect the suppression of the pair potential in the S leads near the interfaces. Our main goal is to study how the equilibrium properties of this system are influenced by the transparency of the SN interfaces and by the presence of a spin-flip mechanism in the diffusive wire. In particular, we want to study (i) the equilibrium density of states (DOS) in the normal wire and (ii) the supercurrent in the SNS system when a superconducting phase difference ϕ is established between the electrodes.

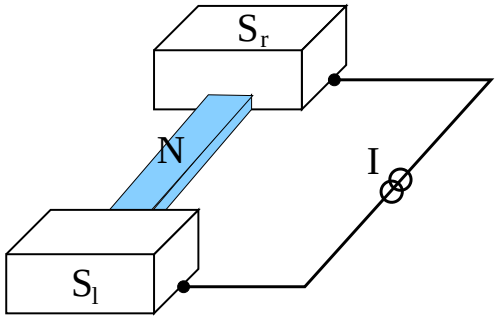

FIG. 1: (Color online) Schematic representation of the system: a metallic diffusive wire (N) is connected at its ends to superconducting reservoirs S_l and S_r. Eventually, a supercurrent I may circulate along the SNS junction.

In order to describe these properties we use the quasiclassical theory of superconductivity in the diffusive limit,[7,32,33] where the mean free path is much smaller than the superconducting coherence length in the normal metal, $\xi = \sqrt{\hbar D/\Delta}$. This theory is formulated in terms of momentum averaged Green's function $\check{\mathbf{G}}(\mathbf{R},\epsilon)$, which depend on position $\mathbf{R}$ and an energy argument ϵ, since we shall only deal with stationary situations. This propagator is a 4×4 matrix in Keldysh space (indicated by an inverted caret), where each entry is a 2×2 matrix in electron-hole space (indicated by a caret)

$$\check{\mathbf{G}} = \begin{pmatrix} \hat{G}^R & \hat{G}^K \\ 0 & \hat{G}^A \end{pmatrix}; \quad \hat{G}^R = \begin{pmatrix} \mathcal{G}^R & \mathcal{F}^R \\ \bar{\mathcal{F}}^R & \bar{\mathcal{G}}^R \end{pmatrix}. \qquad (1)$$

The general definitions of the different functions can be found in Ref. [34]. The Green's functions for the left (l) and right (r) leads can be written as $\check{\mathbf{G}}_j(\epsilon) = e^{-i\phi_j\hat{\tau}_3/2\hbar}\check{\mathbf{G}}_0(\epsilon)e^{i\phi_j\hat{\tau}_3/2\hbar}$, where ϕ_j is the phase of the order parameter of the electrode $j = l, r$. Here, $\check{\mathbf{G}}_0(\epsilon)$ is the equilibrium bulk Green's function of a BCS superconductor. Notice that, since we shall only consider equilibrium situations, the Keldysh component of $\check{\mathbf{G}}(\mathbf{R},\epsilon)$ can be expressed in terms of the retarded and advanced components as $\hat{G}^K = (\hat{G}^R - \hat{G}^A)\tanh(\beta\epsilon/2)$, where $\beta = 1/k_{\rm B}T$ is the inverse of the temperature.

The propagator $\check{\mathbf{G}}(\mathbf{R},\epsilon)$ satisfies the stationary Usadel equation, which in the N region reads[35]

$$\frac{\hbar D}{\pi}\nabla\left(\check{\mathbf{G}}\nabla\check{\mathbf{G}}\right) - \frac{\hbar}{2\pi\tau_{sf}}\left[\check{\tau}_{\mathbf{3}}\check{\mathbf{G}}\check{\tau}_{\mathbf{3}},\check{\mathbf{G}}\right] + \epsilon\left[\check{\tau}_{\mathbf{3}},\check{\mathbf{G}}\right] = 0, \quad (2)$$

where $\check{\tau}_{\mathbf{3}}$ is proportional to the unit matrix in Keldysh space and equal to the Pauli matrix $\hat{\tau}_3$ in electron-hole space. Equation (2) is supplemented by the normalization condition $\check{\mathbf{G}}^2 = -\pi^2\check{\mathbf{1}}$. In the previous equation, τ_{sf} is the scattering time associated to spin-flip (magnetic) impurities or related pair-breaking mechanisms.

For instance, as it has been shown in Refs. [11,31], if the normal wire is a thin film and its width W does not exceed ξ, the effect of a perpendicular magnetic field H can be described with an effective spin-flip scattering rate $\Gamma_{sf} = \hbar/\tau_{sf} = De^2H^2W^2/(6\hbar)$.

In order to solve numerically the Usadel equation it is convenient to use the so-called Riccati parametrization,[36] which accounts automatically for the normalization condition. In this method and for spin-singlet superconductors, the retarded and advanced Green's functions are parametrized in terms of two coherent functions $\gamma^{R,A}(\mathbf{R},\epsilon)$ and $\tilde{\gamma}^{R,A}(\mathbf{R},\epsilon)$ as follows

$$\hat{G}^{R,A} = \mp i\pi \hat{N}^{R,A} \begin{pmatrix} 1-\gamma^{R,A}\tilde{\gamma}^{R,A} & 2\gamma^{R,A} \\ 2\tilde{\gamma}^{R,A} & \tilde{\gamma}^{R,A}\gamma^{R,A}-1 \end{pmatrix} \quad (3)$$

with the "normalization matrices"

$$\hat{N}^{R,A} = \begin{pmatrix} (1+\gamma^{R,A}\tilde{\gamma}^{R,A})^{-1} & 0 \\ 0 & (1+\tilde{\gamma}^{R,A}\gamma^{R,A})^{-1} \end{pmatrix}.$$

Some of these functions are related by fundamental symmetries (particle-hole, retarded-advanced) like

$$\gamma^A(\mathbf{R},\epsilon) = -\left[\tilde{\gamma}^R(\mathbf{R},\epsilon)\right]^* \;;\; \gamma^A(\mathbf{R},\epsilon) = -\gamma^R(\mathbf{R},-\epsilon) \quad (4)$$

Therefore, we just have to determine, for instance, the retarded functions. Using their definition in Eq. (3) and the Usadel equation (2), one can obtain the following transport equations for these functions in the normal wire region[37]

$$\partial_x^2\gamma^R + (\partial_x\gamma^R)\frac{\tilde{\mathcal{F}}^R}{i\pi}(\partial_x\gamma^R) - 2\left(\frac{\Gamma_{sf}}{\epsilon_T}\right)\gamma^R\frac{\tilde{\mathcal{G}}^R}{i\pi} + 2i\left(\frac{\epsilon}{\epsilon_T}\right)\gamma^R = 0 \quad (5)$$

$$\partial_x^2\tilde{\gamma}^R + (\partial_x\tilde{\gamma}^R)\frac{\mathcal{F}^R}{i\pi}(\partial_x\tilde{\gamma}^R) + 2\left(\frac{\Gamma_{sf}}{\epsilon_T}\right)\tilde{\gamma}^R\frac{\mathcal{G}^R}{i\pi} + 2i\left(\frac{\epsilon}{\epsilon_T}\right)\tilde{\gamma}^R = 0. \quad (6)$$

Here, x is the dimensionless coordinate which describes the position along the N wire and ranges from 0 (left lead) to 1 (right lead). The expressions for $\tilde{\mathcal{F}}^R$, $\tilde{\mathcal{G}}^R$, $\mathcal{F}^R$ and $\mathcal{G}^R$ are obtained by comparing Eq. (1) with Eq. (3). Notice that Eqs. (5,6) couple the functions with and without tilde. This means in practice that, in general, one has to solve Eqs. (5,6) simultaneously.

Now, we have to provide the boundary conditions for the Eqs. (5,6). Let us first remind that for ideal interfaces (perfect transparency) such conditions at the ends of the N wire result from the continuity of the Green's functions over the SN interfaces:

$$\begin{aligned} \gamma_l^R(\epsilon) = \gamma_0^R(\epsilon) \;;\; \tilde{\gamma}_l^R(\epsilon) = -\gamma_0^R(\epsilon) \\ \gamma_r^R(\epsilon) = e^{-i\phi}\gamma_0^R(\epsilon - eV) \;;\; \tilde{\gamma}_r^R(\epsilon) = -e^{i\phi}\gamma_0^R(\epsilon + eV) \end{aligned} \quad (7)$$

where $\gamma_l^R(\epsilon) \equiv \gamma^R(x=0,\epsilon)$ and $\gamma_r^R(\epsilon) \equiv \gamma^R(x=1,\epsilon)$, and the same for the coherent function with tilde. Here, $\gamma_0^R(\epsilon) = -\Delta/\{\epsilon^R + i\sqrt{\Delta^2-(\epsilon^R)^2}\}$, where $\epsilon^R = \epsilon + i0^+$. Finally, ϕ is the eventual phase difference between the two superconducting reservoirs, which we assume to be applied in the right electrode.

For non-ideal interfaces one has to use the more general boundary conditions derived in Refs. [38,39]. These conditions for an spin-conserving interface are expressed in terms of the Green's functions as follows

$$\check{\mathbf{G}}^\beta\partial_x\check{\mathbf{G}}^\beta = \left(\frac{G_0}{G_N}\right)\sum_i \frac{2\pi^2\tau_i\left[\check{\mathbf{G}}^\beta,\check{\mathbf{G}}^\alpha\right]}{4\pi^2 - \tau_i\left(\left\{\check{\mathbf{G}}^\beta,\check{\mathbf{G}}^\alpha\right\} + 2\pi^2\right)}. \quad (8)$$

Here, $\check{\mathbf{G}}^{\beta(\alpha)}$ refers to the Keldysh-Green's function on side $\beta(\alpha)$ of the interface, $G_0 = 2e^2/h$ is the quantum of conductance, G_N is the conductance of the normal wire and τ_i are the different transmission coefficients characterizing the interface. In general, one would need the whole set $\{\tau_i\}$, but since one does not have access to this information we adopt here a practical point of view. We assume that all the N interface open channels have the same transmission τ and define $G_B = G_0 N\tau$ as the conductance of the barrier. Thus, the two S-N interfaces will be characterized by two quantities, namely the barrier conductance G_B and the transmission τ, and our starting point for the boundary conditions will be

$$r\check{\mathbf{G}}^\beta\partial_z\check{\mathbf{G}}^\beta = \frac{2\pi^2\left[\check{\mathbf{G}}^\beta,\check{\mathbf{G}}^\alpha\right]}{4\pi^2 - \tau\left(\left\{\check{\mathbf{G}}^\beta,\check{\mathbf{G}}^\alpha\right\} + 2\pi^2\right)}, \quad (9)$$

where we have defined the ratio $r = G_N/G_B$. In this language, an ideal interface is characterized by $r = 0$ and a tunnel contact is described by $\tau \ll 1$. In what follows, unless the opposite is explicitly stated, we shall assume a symmetric situation with two identical interfaces. In the literature the so-called Kupriyanov-Lukichev[23] boundary conditions are often used. These conditions can be obtained from Eq. (9) by removing the term proportional to τ in the denominator. Such approximation is valid strictly speaking for the case of tunnel junctions ($\tau \ll 1$) and it turns out to be very good for highly transparent interfaces ($r \ll 1$).

The next step is to express these boundary conditions directly in terms of the coherent functions. Substituting the definitions of Eq. (3) into Eq. (9) and after straightforward algebra, one obtains the following boundary conditions for the parameterizing functions

$$\mp r\frac{\partial_x\gamma_\beta^R + (\gamma_\beta^R)^2\partial_x\tilde{\gamma}_\beta^R}{(1+\gamma_\beta^R\tilde{\gamma}_\beta^R)^2} = \frac{(1-\gamma_\beta^R\tilde{\gamma}_\beta^R)\gamma_\alpha^R - (1-\gamma_\alpha^R\tilde{\gamma}_\alpha^R)\gamma_\beta^R}{(1+\gamma_\beta^R\tilde{\gamma}_\beta^R)(1+\gamma_\alpha^R\tilde{\gamma}_\alpha^R) - \tau(\gamma_\alpha^R-\gamma_\beta^R)(\tilde{\gamma}_\alpha^R-\tilde{\gamma}_\beta^R)} \quad (10)$$

where the minus sign is for the left interface and the plus sign for the right one. The boundary conditions for $\tilde{\gamma}^R$ can be obtained from Eq. (10) exchanging the quantities without tilde by the corresponding ones with tilde and vice versa. These equations establish a relation between the functions and their derivatives evaluated on the side

of the interface inside the N wire (β) and the corresponding functions evaluated on the side of the interface inside the reservoir (α), which are given by Eq. (7).

In the limit of weak proximity effect, Eqs. (5,6) can solved analytically, as we discuss in Appendix A. However, in general they have to be solved numerically. These are second order differential equations with boundary conditions relating the functions and their derivatives in the two SN interfaces. This is a typical two point boundary value problem that we solve numerically using the so-called relaxation method as described in Ref. [40]. We want to point out that the Riccati parametrization facilitates the numerical calculations because the coherent functions are smooth and bounded. Moreover, this parametrization is also well suited for time-dependent problems, as we have shown in Ref. [41].

To end this section we discuss the formula for the supercurrent. The electrical current can expressed in terms of the Usadel Green's functions as[32]

$$I = \frac{G_{\rm N}}{8\pi^2 e}\int_{-\infty}^{\infty} d\epsilon\ {\rm Tr}\left\{\hat{\tau}_3\left[\check{\mathbf{G}}\partial_x\check{\mathbf{G}}\right]^K(\epsilon)\right\}. \qquad (11)$$

Combining this expression with fundamental symmetries of the Green's functions and using the fact that we only address equilibrium situations, we can write the supercurrent as

$$I = \frac{G_{\rm N}}{e}\int_{-\infty}^{\infty} d\epsilon\ \mathcal{S}(\epsilon)\tanh(\beta\epsilon/2), \qquad (12)$$

where $\mathcal{S} = (1/4\pi^2){\rm Re}\{{\rm Tr}(\hat{\tau}_3\hat{G}^R\partial_x\hat{G}^R)\}$ is the spectral supercurrent.

III. LOCAL DENSITY OF STATES

In equilibrium, the most basic quantity that reflects the proximity effect in the N wire is the local density of states (DOS), which is defined as ${\rm DOS}(x,\epsilon) = -{\rm Im}\left\{\mathcal{G}^R(x,\epsilon)\right\}/\pi$. This quantity can in principle be measured with a tunneling probe electrode as in Ref. [3], or with a scanning tunneling microscope (STM) as in Ref. [4]. In this section we analyze the local DOS in the normal wire in different situations.

Let us start discussing a situation where there is no phase difference between the superconducting reservoirs ($\phi = 0$). In this case, one can show that the relation $\tilde{\gamma}^R(\epsilon) = -\gamma^R(\epsilon)$ holds. Thus, one only needs to solve Eq. (5) for the coherent function $\gamma^R(\epsilon)$. In Fig. 2 we show an example of the local DOS in the middle of a normal wire ($x = 0.5$) of length $L = 2\xi$ without spin-flip scattering ($\Gamma_{sf} = 0$). The most prominent feature is the appearance of a minigap Δ_g in the spectrum, which for perfect transparency scales with the Thouless energy roughly as $\Delta_g \sim 3.1\epsilon_T$ in the long junction limit ($L \gg \xi$). Let us remind that the minigap is the same along the normal wire, although the exact DOS depends on the position. The existence of a minigap in a diffusive normal metal in contact with a superconductor was discussed by McMillan[9]

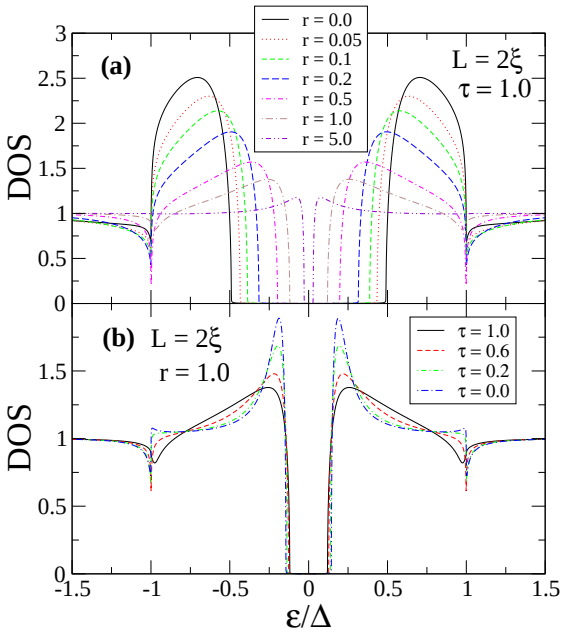

FIG. 2: (Color online) Density of states of a SNS junction as a function of energy in the middle of a wire of length $L = 2\xi$ without spin-flip scattering ($\Gamma_{sf} = 0$). The SN interfaces are assumed to be identical and there is no phase difference between the S electrodes. In panel (a) the different curves correspond to different values of the ratio $r = G_{\rm N}/G_{\rm B}$ and a transmission $\tau = 1$, while in panel (b) they correspond to different values of the transmission τ for a ratio $r = 1.0$.

within a tunneling model, where the normal region was a thin layer. In more recent years, the minigap has been extensively studied in various hybrid diffusive SN and SNS structures.[10,11,12] As one can see in Fig. 2(a), this minigap diminishes progressively as the ratio r increases, i.e. as the interface becomes more opaque. For this particular length, we find that the minigap decays with the interface parameter r as $\Delta_g/\Delta \sim 0.14/r$ for $r > 1$ (see the fit to our numerical data in Fig. 13, Appendix B).

In Fig. 2(b) we illustrate the effect of the transmission coefficient τ in the local DOS for a ratio $r = 1.0$. Notice that the minigap is only slightly reduced as τ decreases, while the features around Δ_g become more pronounced. The effect of a transmission smaller than one is much more pronounced for larger values of r, i.e $r \gg 1$, while for values $r < 1$ it is rather insensitive to the value of τ.

In Fig. 3 we present a detailed study of the decay of the minigap as a function of the wire length for different values of the interface resistance and $\tau = 1.0$. We have normalized the minigap Δ_g with the Thouless energy to show explicitly that in the long wire limit Δ_g simply scales with this energy. In this limit ($\Delta/\epsilon_T \to \infty$) we were able to fit accurately the decay of the minigap with the ratio r with the function $\Delta_g/\epsilon_T = 0.64/(0.20 + r)$ (see Fig. 13 in Appendix B). In the opposite case of a short junction, i.e. when $L \ll \xi$, the minigap is of the order of Δ for perfect transparency, while it is given by

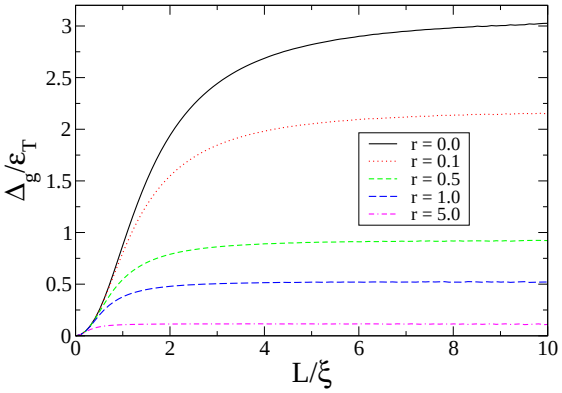

FIG. 3: (Color online) Minigap Δ_g of a SNS junction as a function of the length of the N wire for different values of $r = G_N/G_B$ and $\Gamma_{sf} = 0$. The contact is assumed to be symmetric and the transmission is set to $\tau = 1$. Notice that is Δ_g is normalized by the Thouless energy ϵ_T.

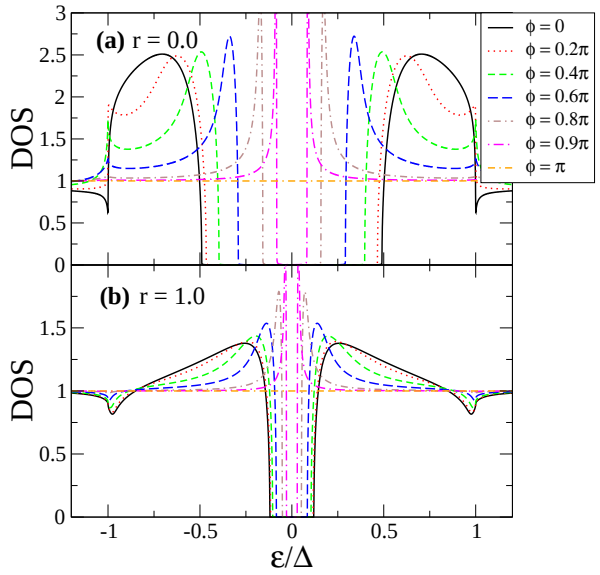

FIG. 4: (Color online) Density of states of a SNS junction as a function of energy in the middle of a wire of length $L = 2\xi$ ($\Gamma_{sf} = 0$) for different values of the superconducting phase difference ϕ. The interfaces are identical and characterized by a ratio $r = G_N/G_B = 0.0$ in panel (a) and $r = 1.0$ in panel (b). In both cases $\tau = 1$.

$\Delta_g \sim \epsilon_T/2r$ in the limit of $r \gg 1$.[24]

Let us now study how the density of states is modified when there is a finite phase difference ϕ between the leads, i.e. in the presence of a supercurrent. In this discussion we shall assume that $\Gamma_{sf} = 0$. Considering ideal interfaces, Zhou *et al.*[12] showed theoretically that the minigap decreases monotonically as the phase difference increases and it closes completely when $\phi = \pi$. In Fig. 4 we show two examples for $L = 2\xi$ of how the DOS in the middle of the wire evolves with the phase ϕ for perfect transparency and $r = 1.0$. Notice that for finite r the qualitative behavior of the minigap is very similar. Indeed, a detailed study shows that, if the minigap is normalized by its value at $\phi = 0$, its phase dependence does not change significantly with the interface resistance. Notice, however, that the features in the DOS around the minigap can be clearly different, as Fig. 4 exemplifies.

Now we turn to the analysis of the influence of spin-flip scattering in the local DOS. Belzig *et al.*[11] showed that the minigap of an SN structure is reduced in the presence of a spin-flip mechanism and vanishes for large values of Γ_{sf}. Different authors[24,29,30] have studied the effect of magnetic impurities in the transport of SN structures and found that the Thouless energy is the scale that controls the effect of spin-flip on the proximity effect. In particular, Crouzy *et al.*[14] have shown analytically that in the long junction limit of an SNS structure, the minigap closes at a critical value of $\Gamma_{sf}^C \approx 4.96\epsilon_T$.

Fig. 5 displays the local DOS in the middle of a normal wire of length $L = 10\xi$ ($\epsilon_T = 0.01\Delta$) for different values of the spin-flip rate Γ_{sf}. The upper panel shows the case of ideal interfaces, while the lower one contains the results for a ratio $r = 1.0$. One can see how the minigap is progressively reduced as Γ_{sf} increases and finally vanishes. For $r = 0$ (perfect interfaces) we find numerically that the gap closes at $\Gamma_{sf}^C \approx 4.9\epsilon_T$ in very good agreement with the long junction limit mentioned above.[14] For the case $r = 1.0$ this critical value is $\Gamma_{sf}^C \approx 0.8\epsilon_T$. This means that it is reduced by approximately a factor 6, which is the same reduction factor obtained for the minigap (see Fig. 3). This indicates that at finite transmission the relevant scale for the proximity effect is the minigap rather than the Thouless energy. This will become even clearer in the analysis of the supercurrent in the next section.

IV. SUPERCURRENT

As mentioned in the introduction, the supercurent in diffusive SNS junctions has been the subject of numerous theoretical and experimental studies. In particular, from the theory side, the results for the critical current for ideal interfaces and without spin-flip scattering are summarized in Refs. [6,25]. The critical current in SNS junctions with partially transparent interfaces was discussed in Ref. [23] using the boundary conditions developed in the same reference. More recently, Heikkilä *et al.*[26] studied the reduction of the zero-temperature critical current with the interface resistance considering a disordered interface.

In this section we shall discuss how both the supercurrent and the critical current are modified by a finite transparency of the interfaces. To be precise, we shall investigate both the current-phase relationship and the temperature dependence of the critical current. Moreover, we shall study in detail the effect of spin-flip scattering in the critical current, which to our knowledge has

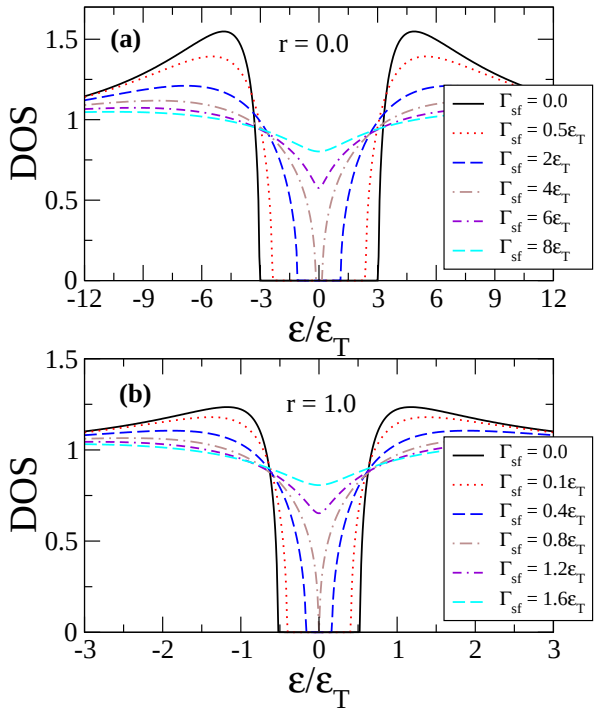

FIG. 5: (Color online) (a) Density of states of a SNS junction as a function of energy in the middle of a wire of length $L = 10\xi$ for $r = 0$ and $\tau = 1.0$. The different curves correspond to different values of the spin-flip scattering rate Γ_{sf}. (b) The same but for $r = 1.0$. Notice that both the energy and the Γ_{sf} are in units of the Thouless energy.

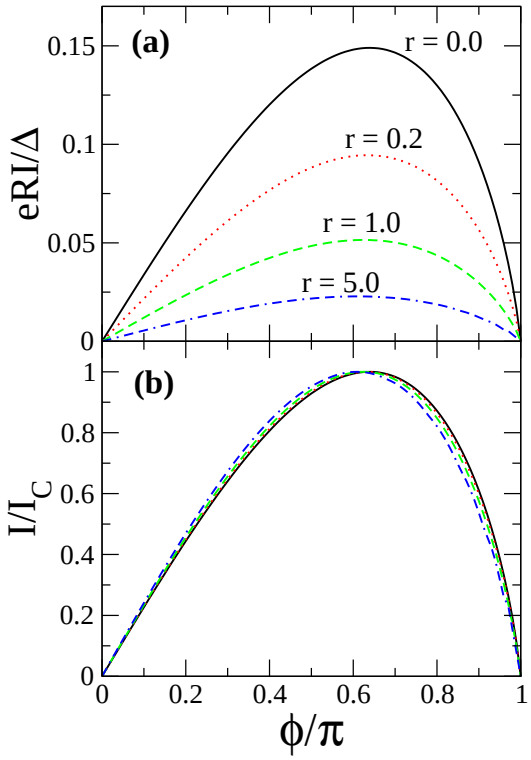

FIG. 6: (Color online) Zero-temperature supercurrent-phase relation of a diffusive SNS junction for $L = 8\xi$ ($\Delta = 64\epsilon_T$) for different values of the ratio $r = G_N/G_B$ and $\tau = 1.0$. In panel (a) we show the results for the product eRI/Δ, where R is the normal-state resistance, while in panel (b) we have normalized the different curves by the critical current I_C.

not been discussed before in the literature. This analysis is very relevant from the experimental point of view, since it might describe the supercurrent in the presence of a magnetic field, as explain in the previous section. Finally, let us remind that the results of this section are complemented with Appendix A, where we study analytically the supercurrent for the case of low transparent interfaces ($r \gg 1$ and $\tau \ll 1$).

We start our discussion by analyzing the current-phase relation in the absence of spin-flip scattering. In Fig. 6 we show this relationship at zero temperature for a wire of $L = 8\xi$ for different values of the ratio r. As it can be seen, the supercurrent is a non-sinusoidal function of the phase difference, which reaches its maximum at $\phi \approx 1.27\pi/2$, almost irrespectively of the value of r. For the ideal case ($r = 0$) this result agrees with the previous results reported in the literature.[6] It is important to stress that in this figure and in what follows we normalize the current with the total resistance in the normal state, R, which includes the contributions of both the diffusive wire and the interfaces. For a symmetric junction this resistance can be expressed in terms of the ratio r as $R = (1 + 2r)/G_N$.

Notice that, as one can see in Fig. 6(b), when the supercurrent is normalized by the critical current I_C, the different results almost collapse into a single curve. At a first glance, this result seems to suggest that the interface transparency just enters as a reduction prefactor in the expression of the critical current. However, as we discuss in the next paragraph, this is clearly not the case at finite temperature.

Let us now turn to the analysis of the temperature dependence of the critical current I_C. In Fig. 7 we show this dependence for a wire of length $L = 8\xi$ and different values of r. Notice that the temperature is normalized with the Thouless energy. The main conclusion that can be extracted from these results is that the critical current decays faster with temperature as the interface resistance increases. Moreover, the saturation region at low temperatures in which the critical current is almost constant shrinks as the interface resistance increases. For ideal interfaces ($r = 0$) this region corresponds, roughly speaking, to the range $k_B T < \epsilon_T$, while for finite r it corresponds to $k_B T < \Delta_g$. This illustrates the fact that is the minigap the scale that controls the magnitude of the supercurrent at arbitrary transparency. The faster decay for partially transparent interfaces can be confirmed analytically in the limit of very long junctions ($\epsilon_T/\Delta \to 0$). In this case and for perfectly transparent interfaces ($r = 0$), one finds a critical

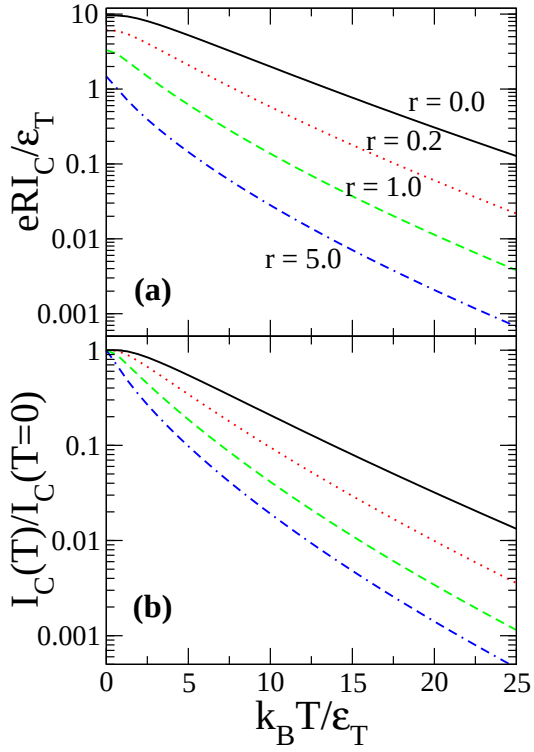

FIG. 7: (Color online) (a) Critical current of a diffusive SNS junction as a function of the temperature for $L = 8\xi$ and different values of the ratio $r = G_N/G_B$ and $\tau = 1.0$. (b) The same but normalized by the critical current at zero temperature.

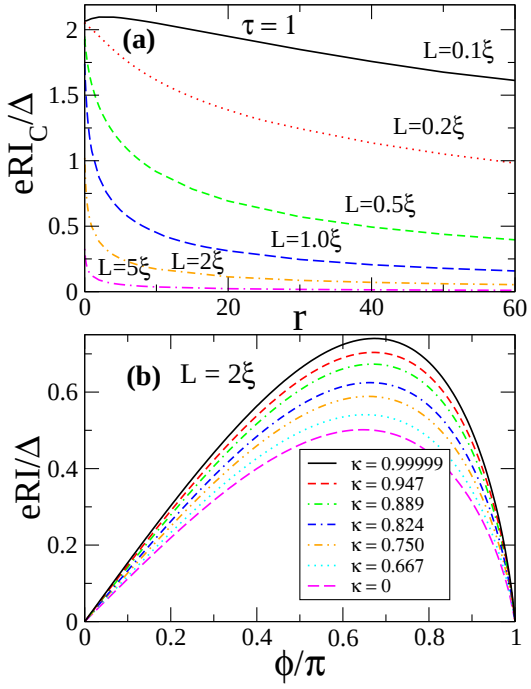

FIG. 8: (Color online) (a) Zero-temperature critical current of a diffusive SNS system with $\tau = 1$ as a function of the parameter $r = G_N/G_B$ for different lengths of the normal wire. (b) Current-phase relation at zero temperature for an asymmetric junction with $L = 2\xi$ and $\tau = 1$. The asymmetry parameter κ is defined as $\kappa = 1 - r_R/r_L$ with $r_R \leq r_L$ and $r_L + r_R = r_{LR} = \text{const}$. Here $r_{LR} = 2$ and $r_L = 1, 1.5, 1.7, 1.8, 1.9, 1.95, 1.99999$

.

current that decays as $I_C \propto (k_B T/\epsilon_T)^{3/2} \exp(-L/L_T)$, where $L_T = \sqrt{\hbar D/2\pi k_B T}$ is the thermal length (see Refs. [6,22]). In the opposite case of opaque interfaces ($r \gg 1$), the result of Appendix A indicates that the critical current decays as $I_C \propto (k_B T/\epsilon_T)^{1/2} \exp(-L/L_T)$.

The decay of the zero-temperature critical current with the interface resistance is examined systematically in Fig. 8(a) for different wire lengths and fixed transmission $\tau = 1$. After normalizing the curves by the resistance in the normal state we find in the limit of very short wires ($L \ll \xi$) a maximal critical current at finite r before it slowly decays for large interface resistances. Thus, $eRI_C \sim \Delta$ in the whole parameter space. For wires with $L \geq \xi$ we find a monotonic decay of eRI_C/Δ with increasing r. Then, for $\Delta/\epsilon_T \to \infty$ the energy scale of the critical current for large ratios r is determined by an effective Thouless energy $\epsilon_{T,\text{eff}}/\epsilon_T \sim A\, r^B/(C + r)$. For instance, when $r \geq 10$ we can fit the decay of the eRI_C product for the special case of a wire with $L = 9\xi$ with the help of $eRI_C/\epsilon_T = 5.13\, r^{0.29}/(0.22 + r)$ (see Fig. 13). Here a fitting curve with $B = 0$ would be proportional to the minigap but would only give a rough estimate of $eRI_C(r)$. So far we do not have a good explanation of the factor r^B and the numerical value of B.

The lower panel of Fig. 8 shows the current-phase relation at zero-temperature for a junction with $L = 2\xi$, $\tau = 1$ and asymmetric barriers as a function of the asymmetry parameter $\kappa = 1 - r_L/r_R$ that fulfills $r_L + r_R = r_{LR} = const$. The critical current shows an enhancement for larger asymmetries while the phase difference moves towards π as κ increases. By modeling the diffusive SNS junction as a point contact and averaging the current through the different channels over the bimodal distribution for diffusive systems, one can understand this trend with the help of the Kirchhoff rules and the set of possible shapes of the current-phase relation in this regime.[25] Furthermore, the formulas of the Appendix A can be generalized to the asymmetric case. Then, the eRI_C product, Eq. (A9), is proportional to $(r_L + r_R)/(r_L r_R)$ what is in agreement with our numerical results.

Let us now discuss the influence of a spin-flip mechanism in the supercurrent. As explained above, the spin-flip scattering may be due to paramagnetic impurities and in this case Γ_{sf} is proportional to the impurity concentration, or it may be caused by a magnetic field and in this case Γ_{sf} is proportional to the square of the field. Indeed, this second possibility is much more interesting since it offers a natural way to control the strength of the spin-flip scattering and, in this sense, it is also more relevant from the experimental point of view.

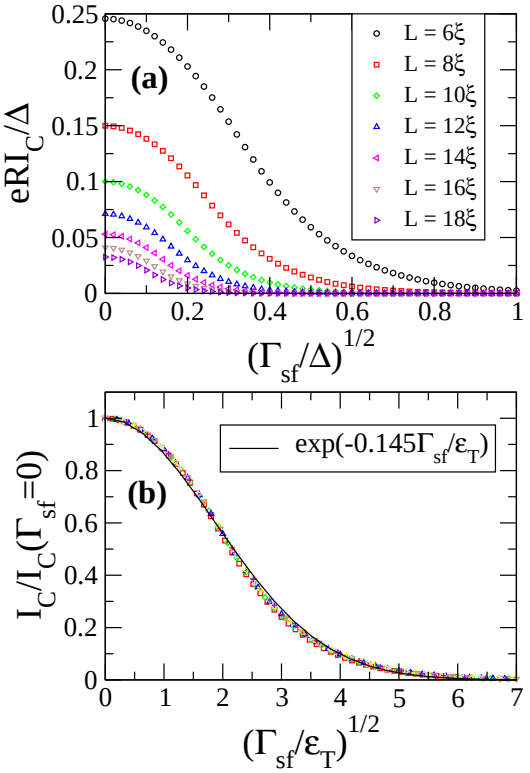

FIG. 9: (Color online) (a) Zero-temperature critical current of a diffusive SNS as a function of the spin-flip rate for different lengths of the normal wire and ideal interfaces ($r = 0$). (b) The same but the critical current is now normalized by the zero spin-flip rate value and Γ_{sf} is normalized by the Thouless energy of the wires. Notice that all the curves collapse into a single one that can be approximately described by the Gaussian function $I_C/I_C(\Gamma_{sf} = 0) = \exp(-0.145\Gamma_{sf}/\epsilon_T)$ shown as a back solid line.

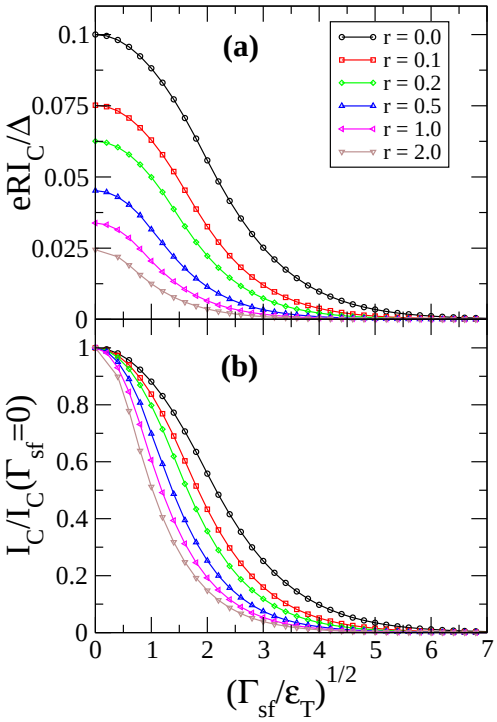

FIG. 10: (Color online) (a) Zero-temperature critical current for a wire length $L = 10\xi$ as a function of the spin-flip rate for different values of the interface resistance and $\tau = 0$. (b) The same as in the upper panel, but the critical current is normalized by its value at $\Gamma_{sf} = 0$.

Fig. 9 displays the zero-temperature critical current as a function of the spin-flip rate Γ_{sf} for different values of the wire length and ideal interfaces ($r = 0$). The reason for plotting the current as a function of the square root of the rate is that this plot can be seen as the magnetic field dependence of the critical current when the normal wire is a thin film. It is important to remark that in these calculations we assume that the order parameter in the leads is not affected by the spin-flip mechanism (such an effect can be trivially included). As one can see in Fig. 9 the spin-flip mechanism causes a decay of the critical current. It is well-known[27,28] that the spin-flip scattering acts as a pair-breaking mechanism for the Cooper pairs that penetrate in the normal wire. Such scattering introduces a new relevant length scale in the problem, namely the spin-flip length $L_{sf} = \sqrt{\hbar D/2\Gamma_{sf}}$. When this length becomes smaller than the length of the system and the thermal length, it dominates the decay of the supercurrent. As we show in Fig. 9(b), when I_C its normalized by its value in the absence of spin-flip rate, its decay with Γ_{sf} becomes universal for relatively long wires. Such decay can be phenomenologically fitted with a Gaussian function $I_C/I_C(\Gamma_{sf} = 0) = \exp(-0.145\Gamma_{sf}/\epsilon_T)$, as demonstrated in Fig. 9(b). The analysis detailed in Appendix A suggests that, in the low transparent regime, the decay follows a law of the type $I_C \propto (\epsilon_T/2\Gamma_{sf})^{1/2} \exp(-L/L_{sf})$ at finite temperature, which numerically is similar to the Gaussian function above.

On the other hand, as one can see in Fig. 9, there is still a non-negligible supercurrent even when minigap is completely closed, i.e. when $\Gamma_{sf} > 5\epsilon_T$. This phenomenon in the proximity structure considered here is the equivalent of the well-known gapless superconductivity in bulk superconductors.[27,28]

In order to understand the role of the interface transparency in the decay of the critical current as a function of Γ_{sf}, we present in Fig. 10 the results for I_C for a wire of length $L = 10\xi$ for different values of the ratio r. As it can be seen in particular in Fig. 10(b), the critical current decays faster as the interface resistance increases. This fact illustrates again that the most relevant energy scale at finite transparency is the minigap rather than the Thouless energy.

Finally, to complete the discussion of the role of the spin-flip scattering, let us now describe what happens at finite temperatures. In Fig. 11 one can see the critical current for a wire length $L = 10\xi$ as a function of the

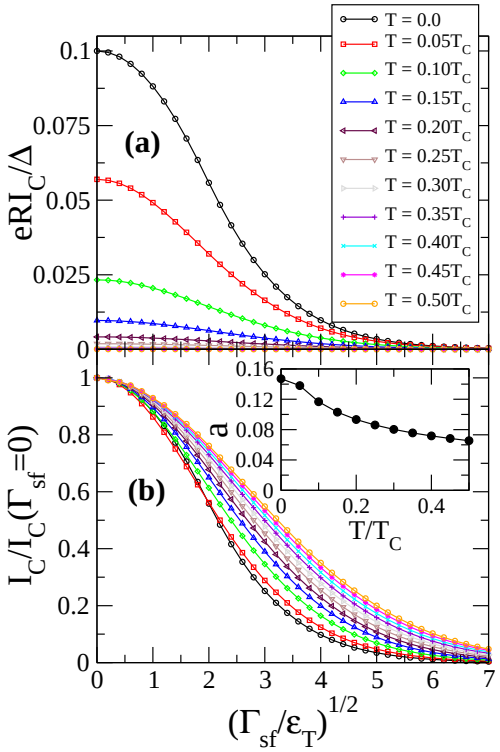

FIG. 11: (Color online) (a) Critical current for a wire length $L = 10\xi$ as a function of the spin-flip rate for different values of the temperature (in unit of the critical temperature, T_C). (b) The same as in the upper panel, but the critical current is normalized by its value at $\Gamma_{sf} = 0$. The inset show the temperature dependence of the constant a used in the Gaussian fits: $I_C/I_C(\Gamma_{sf} = 0) = \exp(-a\Gamma_{sf}/\epsilon_T)$.

rate Γ_{sf} for different values of the temperature. The main conclusion is that by increasing the temperature the decay of the critical current becomes slower. Such a trend can be understood with the help of the result of Appendix A.

V. CONCLUSIONS

With the advances in the fabrication techniques of superconducting hybrid structures and the development of local measuring probes, it is now possible to explore the proximity effect in diffusive metallic nanostructures in great detail. In this sense, it is highly desirable from the theory side to elucidate the role of ingredients usually present in experiments such as partially transmissive interfaces and pair-breaking mechanisms. With this idea in mind, we have presented in this work a detailed analysis of the density of states and supercurrent in diffusive SNS junctions. In particular, we have studied the influence in these two equilibrium properties of an arbitrary transmission of the interfaces and spin-flip scattering in the normal wire. Our analysis is based on the quasiclassical theory for diffusive superconductors (Usadel theory), supplemented by the boundary conditions put forward by Nazarov.[38]

With respect to the local density of states, we have shown that the minigap that appears in the normal wire is very sensitive to the interface transmission both in the absence and in the presence of a supercurrent in the system. Moreover, we have shown that the minigap closes when the energy rate that describes the spin-flip scattering is a few times larger than the minigap in the absence of this type of scattering. This fact nicely illustrates that the minigap is indeed the relevant energy scale for the proximity effect for non-ideal interfaces.

Turning to the analysis of the supercurrent, we have shown that both the magnitude and temperature dependence of the critical current depend crucially on the interface resistance. In particular, the critical current decays faster with temperature as the interface resistance increases. Moreover, we have studied how the existence of spin-flip scattering in the normal wire diminishes the supercurrent and identified the relevant energy and length scales for its decay. In particular, we have shown that a supercurrent can still flow when the minigap is completely closed, which is the analogous in proximity structures of the well-known gapless superconductivity in bulk samples.[27,28] This prediction can be tested experimentally by using an external magnetic field, as long as the width of the normal wire is smaller or comparable to the superconducting coherence length ad it is made of a thin film.[11,31]

Acknowledgments

It is a pleasure to acknowledge numerous and fruitful discussions with Sophie Guéron, Hélène Bouchiat, Francesca Chiodi and Meydi Ferrier, and Philippe Joyez and Hélène Le Sueur. We also want to thank them for showing us the results of their respective experiments before publication. We also want to thank Andrei Zaikin, Gilles Montambaux, Tero Heikkilä, Christoph Strunk and Franziska Rohlfing for useful discussions. F.S.B. acknowledges funding by the Ramón y Cajal program. The work by J.C.H. and W.B. was funded by the DFG through SFB 513. J.C.C. and F.S.B. acknowledge financial support by the Spanish CYCIT (contract FIS2005-06255).

APPENDIX A: LINEARIZED EQUATIONS

In the limit of very low transparent interfaces ($r \gg 1$ and $\tau \ll 1$), the supercurrent can be computed analytically by linearizing the Usadel equations.[23] In this appendix we describe how this can be done within the formalism presented in section II.

Assuming that the proximity effect in the normal wire is weak, the coherent functions are small and the retarded

and advanced Green's functions can be approximated by (see Eq. 3)

$$\hat{G}^{R,A} \approx \mp i\pi \begin{pmatrix} 1 & 2\gamma^{R,A} \\ 2\tilde{\gamma}^{R,A} & -1 \end{pmatrix}. \quad \text{(A1)}$$

Here, the coherent functions γ^R and $\tilde{\gamma}^R$ fulfill the linearized version of Eqs. (5,6), which reduce to

$$\partial_x^2\gamma^R + 2\left(\frac{i\epsilon - \Gamma_{sf}}{\epsilon_T}\right)\gamma^R = 0 \quad \text{(A2)}$$

$$\partial_x^2\tilde{\gamma}^R + 2\left(\frac{i\epsilon - \Gamma_{sf}}{\epsilon_T}\right)\tilde{\gamma}^R = 0. \quad \text{(A3)}$$

Notice that now the equations for γ^R and $\tilde{\gamma}^R$ are uncoupled and have an identical form.

The boundary conditions for the previous equations are obtained by linearizing Eq. (10) in the following way

$$\mp r\partial_x\gamma_\beta^R = \frac{\gamma_\alpha^R}{1+\gamma_\alpha^R\tilde{\gamma}_\alpha^R} = -\frac{\mathcal{F}_\alpha^R}{2\pi i} \quad \text{(A4)}$$

$$\mp r\partial_x\tilde{\gamma}_\beta^R = \frac{\tilde{\gamma}_\alpha^R}{1+\tilde{\gamma}_\alpha^R\gamma_\alpha^R} = -\frac{\tilde{\mathcal{F}}_\alpha^R}{2\pi i}, \quad \text{(A5)}$$

where the minus sign is for the left interface and the plus sign for the right one. Here, $\mathcal{F}_\alpha^R$ and $\tilde{\mathcal{F}}_\alpha^R$ are the anomalous Green's functions of the corresponding superconducting lead $\alpha = l, r$.

The solution of Eq. (A2) with the boundary conditions of Eq. (A4) can be written as

$$\gamma^R(x) = A^R e^{i\lambda x} + B^R e^{-i\lambda x}, \quad \text{(A6)}$$

where $\lambda^2 = 2(i\epsilon - \Gamma_{sf})/\epsilon_T$ and the constants A^R and B^R can be expressed as

$$A^R = \frac{1}{4\pi i r\lambda\sin\lambda}\left(\mathcal{F}_r^R + \mathcal{F}_l^R e^{-i\lambda}\right)$$

$$B^R = \frac{1}{4\pi i r\lambda\sin\lambda}\left(\mathcal{F}_r^R + \mathcal{F}_l^R e^{i\lambda}\right).$$

The solution for the function $\tilde{\gamma}^R$ is obtained from the solution for γ^R by replacing the functions $\mathcal{F}_{r,l}^R$ by $\tilde{\mathcal{F}}_{r,l}^R$.

After linearizing the expression of Eq. (12), the supercurrent can be written as

$$I = \frac{G_N}{e}\int_{-\infty}^{\infty} d\epsilon\ \mathrm{Re}\left\{\tilde{\gamma}^R\partial_x\gamma^R - \gamma^R\partial_x\tilde{\gamma}^R\right\}\tanh\left(\frac{\beta\epsilon}{2}\right). \quad \text{(A7)}$$

Using the solutions for γ^R and $\tilde{\gamma}^R$, it is straightforward to show that the supercurrent-phase relation can be written as

$$I = \frac{G_N}{e\pi^2 r^2}\sin(\phi)\int_{-\infty}^{\infty} d\epsilon\ \mathrm{Re}\left\{\frac{-(\mathcal{F}_S^R)^2}{2i\lambda\sin\lambda}\right\}\tanh\left(\frac{\beta\epsilon}{2}\right), \quad \text{(A8)}$$

where $\mathcal{F}_S^R$ is the bulk anomalous Green's function without including the superconducting phase. This integral

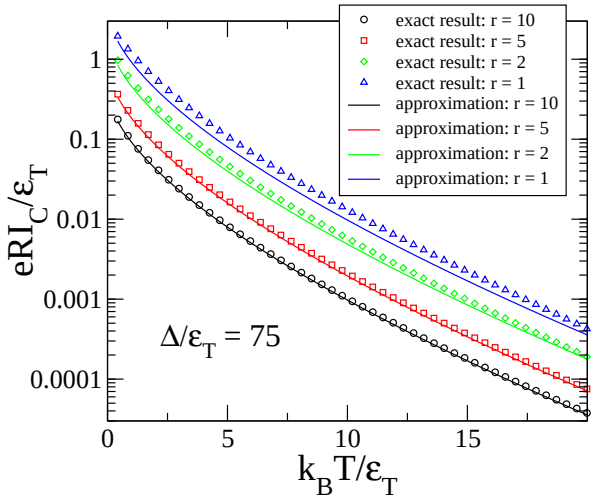

FIG. 12: (Color online) Comparison between the linearized result of Eq. (A9) and the exact numerical result for the temperature dependence of the critical current for a wire with $\epsilon_T = 75\Delta$ in the absence of spin-flip scattering ($\Gamma_{sf} = 0$). The different curves correspond to different values of the ratio $r = G_N/G_B$ and in the exact result we have used $\tau = 0$.

can be done analytically and the result for the critical current is

$$eRI_C = \frac{4\pi k_B T}{r}\sum_{n=0}^{\infty}\frac{\Delta^2/(\Delta^2+\omega_n^2)}{\sqrt{2\left(\frac{\omega_n+\Gamma_{sf}}{\epsilon_T}\right)}\sinh\left(\sqrt{2\left(\frac{\omega_n+\Gamma_{sf}}{\epsilon_T}\right)}\right)}, \quad \text{(A9)}$$

where $\omega_n = (2n+1)\pi k_B T$. Here, we have used $R = (1+2r)/G_N \approx 2r/G_N$. If in particular the temperature is just a few times larger than the Thouless energy, one just need to keep the first term ($n = 0$) in the previous expression. In the limit of an infinitely long wire this formula reduces to

$$eRI_C = \frac{4\pi k_B T}{r}\left(\frac{\tilde{L}}{L}\right)\exp(-L/\tilde{L}), \quad \text{(A10)}$$

where the effective length $\tilde{L} = L_T L_{sf}/\sqrt{L_T^2 + L_{sf}^2}$. Here, $L_T = \sqrt{\hbar D/2\pi k_B T}$ is the thermal length and $L_{sf} = \sqrt{\hbar D/2\Gamma_{sf}}$ is the spin-flip length.

In order to establish the range of validity of the expression of Eq. (A9) we have compared this result with the full numerical solution of the non-linearized Usadel equations. An example of such a comparison for the temperature dependence of the critical current is presented in Fig. 12 for a wire with $\epsilon_T = 75\Delta$. The different curves correspond to different values of the ratio $r = G_N/G_B$ keeping always $\tau = 0$, which correspond to a tunnel junction. Notice that the approximation of Eq. (A9) describes very well the exact results even for values of r very close to 1.

In the limit of highly transparent interfaces, i.e. $r \ll 1$, the solution of Eqs. (5,6) demands a more careful

treatment.[22] However, in the limit of high temperatures ($k_BT \gg \Delta$) one can obtain an analytical expression for the critical current using the linearized solution of Eq. (A6) and assuming that this function is continuous at the SN interfaces. This means in practice that the constants A^R and B^R appearing Eq. (A6) adopt now the following form

$$A^R = \frac{1}{2i\sin\lambda}\left(\gamma_r^R - \gamma_l^R e^{-i\lambda}\right)$$
$$B^R = \frac{1}{2i\sin\lambda}\left(\gamma_l^R e^{i\lambda} - \gamma_r^R\right).$$

The rest of the calculation is identical and now the result for the critical current is

$$eRI_c = 4\pi k_B T\left(\frac{L}{\tilde{L}}\right)\exp(-L/\tilde{L}). \qquad \text{(A11)}$$

In the absence of spin-flip scattering this result reproduces the well-known result originally derived by Likharev in Ref. [21], which indicates that $I_C \propto (k_BT/\epsilon_T)^{3/2}\exp(-L/L_T)$. It has been shown that this dependence describes a broad temperature range,[6,22] as long as $k_BT \gg \epsilon_T$.

APPENDIX B: NUMERICAL FITS

Fig. 13 shows some of the numerical fits mentioned in sections III and IV.

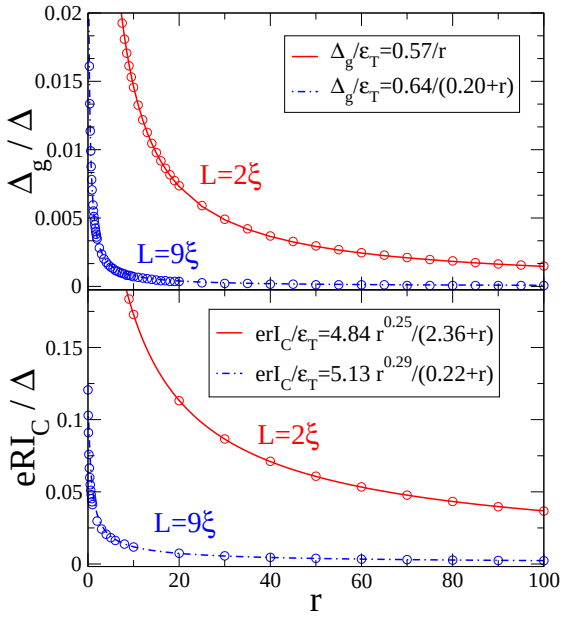

FIG. 13: (Color online) Minigap and critical supercurrent as a function of r for the two lengths $L = 2\xi$ and $L = 9\xi$. The solid lines show the fitting-curves of the numerically calculated data (circles) in units of the Thouless energy for $r \gg 1$.

[1] P.G. de Gennes, Rev. Mod. Phys. **36**, 225 (1964).
[2] B. Pannetier and H. Courtois, J. Low Temp. Phys. **188**, 599 (2000).
[3] S. Guéron, H. Pothier, N.O. Birge, D. Esteve, and M.H. Devoret, Phys. Rev. Lett. **77**, 3025 (1996).
[4] N. Moussy, H. Courtois and B. Pannetier, Europhys. Lett. **55**, 861 (2001).
[5] H. Courtois, P. Charlat, Ph. Gandit, D. Mailly, and B. Pannetier, J. Low Temp. Phys. **116**, 187 (1999).
[6] P. Dubos, H. Courtois, B. Pannetier, F.K. Wilhelm, A.D. Zaikin, and G. Schön, Phys. Rev. B **63**, 064502 (2001).
[7] K.D. Usadel, Phys. Rev. Lett. **25**, 507 (1970).
[8] A.F. Andreev, Sov. Phys. JETP **19**, 1228 (1964).
[9] W.L. McMillan, Phys. Rev. **175**, 537 (1968).
[10] A.A. Golubov and M.Yu Kupriyanov, J. Low Temp. Phys. **70**, 83 (1988); JETP Lett. **61**, 830 (1995).
[11] W. Belzig, C. Bruder and G. Schön, Phys. Rev. B **54**, 9443 (1996).
[12] F. Zhou, P. Charlat, B. Spivak, and B. Pannetier, J. Low. Temp. Phys. **110**, 841 (1998).
[13] D.A. Ivanov, R. von Roten, and G. Blatter, Phys. Rev. B **66**, 052507 (2002).
[14] B. Crouzy, E. Bascones, and D.A. Ivanov, Phys. Rev. B **72**, 092501 (2005).
[15] E. Scheer, W. Belzig, Y. Naveh, M.H. Devoret, D. Esteve, and C. Urbina, Phys. Rev. Lett. **86**, 284 (2001).
[16] G. Rubio-Bollinger, C. de las Heras, E. Bascones, N. Agraït, F. Guinea, and S. Vieira, Phys. Rev. B **67**, 121407(R) (2003).
[17] J. Clarke, Proc. Roy. Soc. A **308**, 447 (1969).
[18] J. G. Shepherd, Proc. Roy. Soc. A **326**, 421 (1972).
[19] J. Warlaumont, J. C. Brown and R. A. Buhrman, Appl. Phys. Lett. **34**, 415 (1979).
[20] R. B. van Dover, A. de Lozanne and M. R. Beasley, J. Appl. Phys. **52**, 7327 (1981).
[21] K. K. Likharev, Sov. Tech. Phys. Lett. **2**, 12 (1976).
[22] A. D. Zaikin and G. F. Zharkov, Sov. J. Low Temp. Phys. **7**, 184 (1981).
[23] M.Yu. Kupriyanov and V.F. Lukichev, Sov. Phys. JETP **67**, 1163 (1988).
[24] A.F. Volkov, A.V. Zaitsev, and T.M. Klapwijk, Physica C **210**, 21 (1993).
[25] For a complete list of references, see A.A. Golubov, M. Yu. Kupriyanov, and E. Il'ichev, Rev. Mod. Phys. **76**, 411 (2004).
[26] T.T. Heikkilä, J. Särkkä, and F.K. Wilhelm, Phys. Rev. B **66**, 184513 (2002).
[27] A. Abrikosov, L. Gor'kov, and I.Y. Dzyaloshinskii, *Quantum Field Theoretical Methods in Statistical Physics* (Pergamon Press, New York, 1965).
[28] K. Maki, *Superconductivity*, (Marcel Dekker, Inc., New York, 1966) Vol. II.

[29] S. Yip, Phys. Rev. B **52**, 15504 (1995).
[30] T. Yokoyama, Y. Tanaka, A.A. Golubov, J. Inoue, and Y. Asano, Phys. Rev. B **71**, 094506 (2005).
[31] A. Anthore, H. Pothier, and D. Esteve, Phys. Rev. Lett. **90**, 127001 (2003).
[32] A.I. Larkin and Yu.N. Ovchinnikov, in *Nonequilibrium Superconductivity*, edited by D.N. Langenberg and A.I. Larkin (Elsevier, Amsterdam), pag. 493 (1986).
[33] W. Belzig, F. K. Wilhelm, C. Bruder, G. Schön and A.D. Zaikin, Superlattices Microstruct. **25**, 1251 (1999).
[34] J.W. Serene and D. Rainer, Phys. Rep. **101**, 221 (1983).
[35] We assume zero pair interaction in the N region.
[36] M. Eschrig, Phys. Rev. B **61**, 9061 (2000).
[37] M. Eschrig, J. Kopu, A. Konstandin, J.C. Cuevas, M. Fogelström, and G. Schön, Adv. in Solid State Phys. **44**, 533 (2004).
[38] Yu.V. Nazarov, Superlatt. and Microstruct. **25**, 121 (1999).
[39] J. Kopu, M. Eschrig, J.C. Cuevas, and M. Fogelström, Phys. Rev. B **69**, 094501 (2004).
[40] W.H. Press *et al.*, *Numerical Recipes* (Cambridge University Press, 1992).
[41] J.C. Cuevas, J.C. Hammer, J. Kopu, J.K. Viljas, and M. Eschrig, Phys. Rev. B **73**, 184505 (2006).